Supplementary Information

Electrical response and biodegradation of Sepia melanin-shellac films printed on paper

Anthony Camus[1†], Shinhyeong Choe[2†], Camille Bour-Cardinal[1], Joaquin Isasmendi[1], Yongjun Cho[2], Youngju Kim[2], Cristian Vlad Irimia[3], Cigdem Yumusak[3], Mihai Irimia-Vladu[3], Denis Rho[4*], Jaewook Myung[2*], Clara Santato[1*]

[1]Engineering Physics Department, Polytechnique Montréal, 2900 Édouard Montpetit, H3T 1J4, Montréal, Québec, Canada

[2]Department of Civil and Environmental Engineering, KAIST, Daejeon 34141, Republic of Korea

[3]Linz Institute for Organic Solar Cells (LIOS), Institute of Physical Chemistry, Johannes Kepler University Linz, Altenberger Str. Nr. 69, 4040 Linz, Austria

[4]Consultant Biotech, Montreal, Canada (retiree NRC Researcher, Montreal, Canada)

[†]These authors have contributed equally to this work and share the first authorship

*Corresponding Authors: Clara Santato; Jaewook Myung; Denis Rho

Email: clara.santato@polymtl.ca; jjaimyung@kaist.ac.kr; rho.denis29@gmail.com

Supplementary methods:

Thickness

Sepia melanin-shellac printed film thickness was measured with a micrometer *49-86 TMI* (*Testing Machine*) according to the standard TAPPI T-411 (hammer speed of 1 mm/s and pressure of 50 kPa) with an incertitude of 1 µm. Three measurements were made on each sample, at different position.

LDPE sheet thickness was measured with a Mitutoyo 700-118-20 Quick Mini Digital thickness gauge. The result was an average of ten respective measurements.

Elemental Analysis (EA)

The carbon content of dry samples was determined through a FLASH 2000 series elemental analyzer (Thermo Fisher Scientific, MA, USA). The results were an average of 5 respective measurements.

Calculation of mineralization and model

Respired CO_2 from each vessel was captured with $Ba(OH)_2$ scrubbing solution according to the following neutralization reaction, which occurs in an equimolar ratio:

$$Ba(OH)_2 + CO_2 \rightarrow BaCO_3 + H_2O$$

The mass of produced CO_2 (m_c) was calculated by substituting the volume of HCl solution at the equivalence point (V_a) into the following equation:

$$m_c = \left(V_{b,i} \cdot C_{b,i} - \frac{V_a \cdot C_a}{2} \cdot \frac{V_{b,f}}{V_{b,a}} \right) \times 44$$

where the first term indicates initial moles of the $Ba(OH)_2$, and the second term denotes consumed moles of $Ba(OH)_2$ calculated by the volume of HCl titrant at the present end point (pH 8.2)

{

$V_{b,i}$: initial volume of $Ba(OH)_2$ solution (mL)

$V_{b,f}$: final volume of $Ba(OH)_2$ solution (mL)

$V_{b,a}$: aliquot volume of $Ba(OH)_2$ solution (mL)

V_a: volume of HCl solution at the equivalence point (mL)

$C_{b,i}$: initial concentration of $Ba(OH)_2$ solution (M)

C_a: concentration of HCl solution (M)

}

Subsequently, net CO_2 production associated with biodegradation was obtained by subtracting the respired CO_2 of reference vessel from produced CO_2 of sample vessel at each measurement. Finally, the mineralization level was computed by dividing produced CO_2 by the theoretical CO_2 of each sample using the following equation:

$$Mineralization\ (\%) = \frac{m_{c,n}}{m_{c,i}} \times 100$$

Here, $m_{c,n}$ refers to the net cumulative CO_2 in milligrams. The $m_{c,i}$ represents the theoretical maximum CO_2 production calculated from the carbon content of the samples, which was determined via EA 1112 elemental analyzer (Thermo Fisher Scientific, MA, USA).

The biodegradation behavior of Sepia melanin-shellac printed film was evaluated using a first-order decay model as follows:

$$m_{c,n} = m_{c,i}(1 - e^{-kt})$$

Where the t denotes the time of incubation (d) and k indicates rate constant (d^{-1}).

Supplementary note:

Outliers' data analysis

We undertook a statistical analysis of all raw data. This led us to identify three 'outliers' (as explained below), with one associated with the 'reference compost' altering the outcome of the mineralization levels of all test materials.

The original triplicates of the cumulative respired CO_2 data for the five tested conditions are presented in Supplementary figures 13 and 14. In Supplementary figure 13, we have identified the three outliers for Sepia Melanin (A), Shellac (B), and Reference Compost (C), marked in red. Outliers represent dataset (here of Respired CO_2) that differ significantly from the other measurements. Consequently, these outliers were excluded from the calculation of their averages and standard deviations. For the Printed films and Cellulose, no 'outliers' were observed (Supplementary figure 14). The explanation for their exclusion is provided below.
From the data in Supplementary figures 13 and 14, we calculated the averages and standard deviations for each condition at the 85-day endpoint, excluding the outliers. These calculated values were then transferred to Supplementary figure 15 and Supplementary table 3.
The averages observed here (Supplementary figure 15), reported in Supplementary table 3, were used to calculate the mineralization levels included in the revised version of the manuscript.

Overall, the rational for excluding the outliers is based on two main points:

Firstly, Supplementary figure 15 guides the understanding of how we have identified outliers. The figure illustrates, for each type of sample tested (Sepia Melanin, Shellac, Printed film, Cellulose and Reference), the cumulative respired CO_2 after an incubation of 85 d in terms of average with standard deviations. Notably, the three outliers are highlighted in red for Sepia Melanin, Shellac, and Reference Compost, while there are no outliers for Printed films and Cellulose.

Secondly, we identified the outlier nature of the excluded datasets through three key observations that set them apart from their respective duplicate datasets: firstly, (Supplementary figure 13 A) a dataset similar to the reference compost dataset; secondly, (Supplementary figure 13 B) a near-zero respiration signifying a lack of response from this specific bioreactor; and thirdly, (Supplementary figure 13 C) a trend (*e.g.*, slope) inexplicably exceeding that of its respective duplicate dataset.

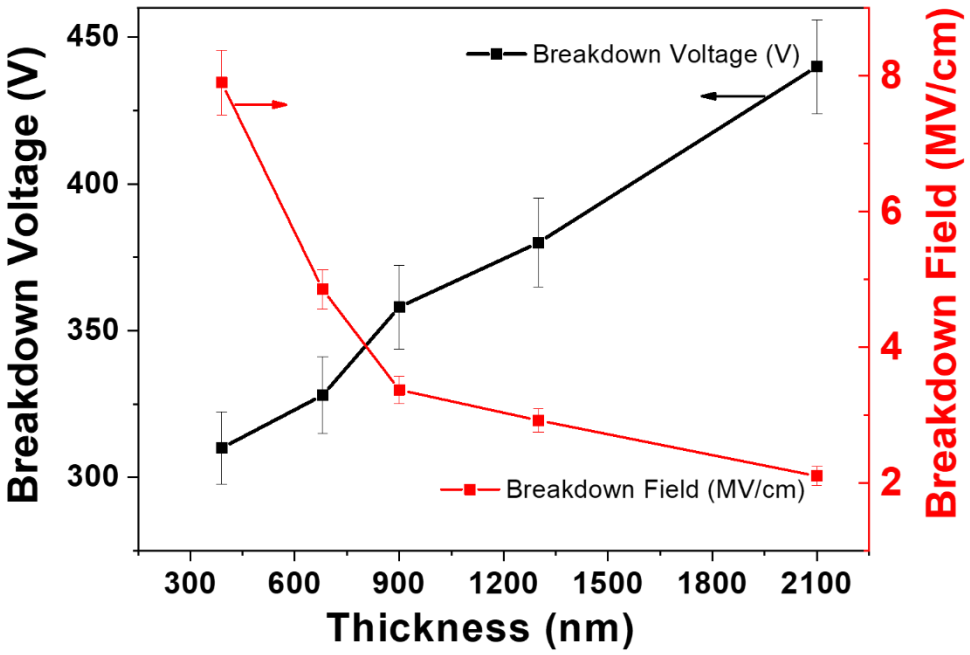

Supplementary Figure 1. Breakdown voltage (black curve) and breakdown field (red curve) measurement as function of the thickness of the shellac layer.

A)

Equivalent circuit before hydration

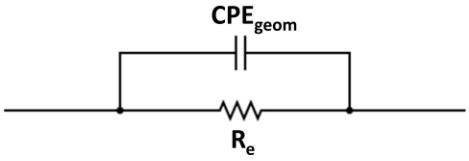

Equivalent circuit after hydration

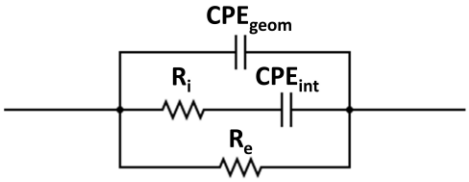

B)

Element		Value
R_e (kΩ)		18.4
CPE_{geom}	C ($nF.s^{\alpha-1}$)	1.3
	α	0.814
R_e (kΩ)		21.9
CPE_{geom}	C ($nF.s^{\alpha-1}$)	26.9
	α	0.647
R_i (kΩ)		87.5
CPE_{int}	C ($\mu F.s^{\alpha-1}$)	12.0
	α	0.402

Supplementary Figure 2. A) Equivalent circuit models of IS data. B) Data used to fit the Nyquist plots of Sepia-shellac films before and after hydration. R_e and R_i are the electronic and ionic resistances, CPE_{geom} and CPE_{int}, are the constant phase elements representing the geometrical and interfacial capacitances of the system. Constant phase elements have an impedance given by: $Z(w) = \frac{1}{(j\omega)^{\alpha}C_{\alpha}}$.

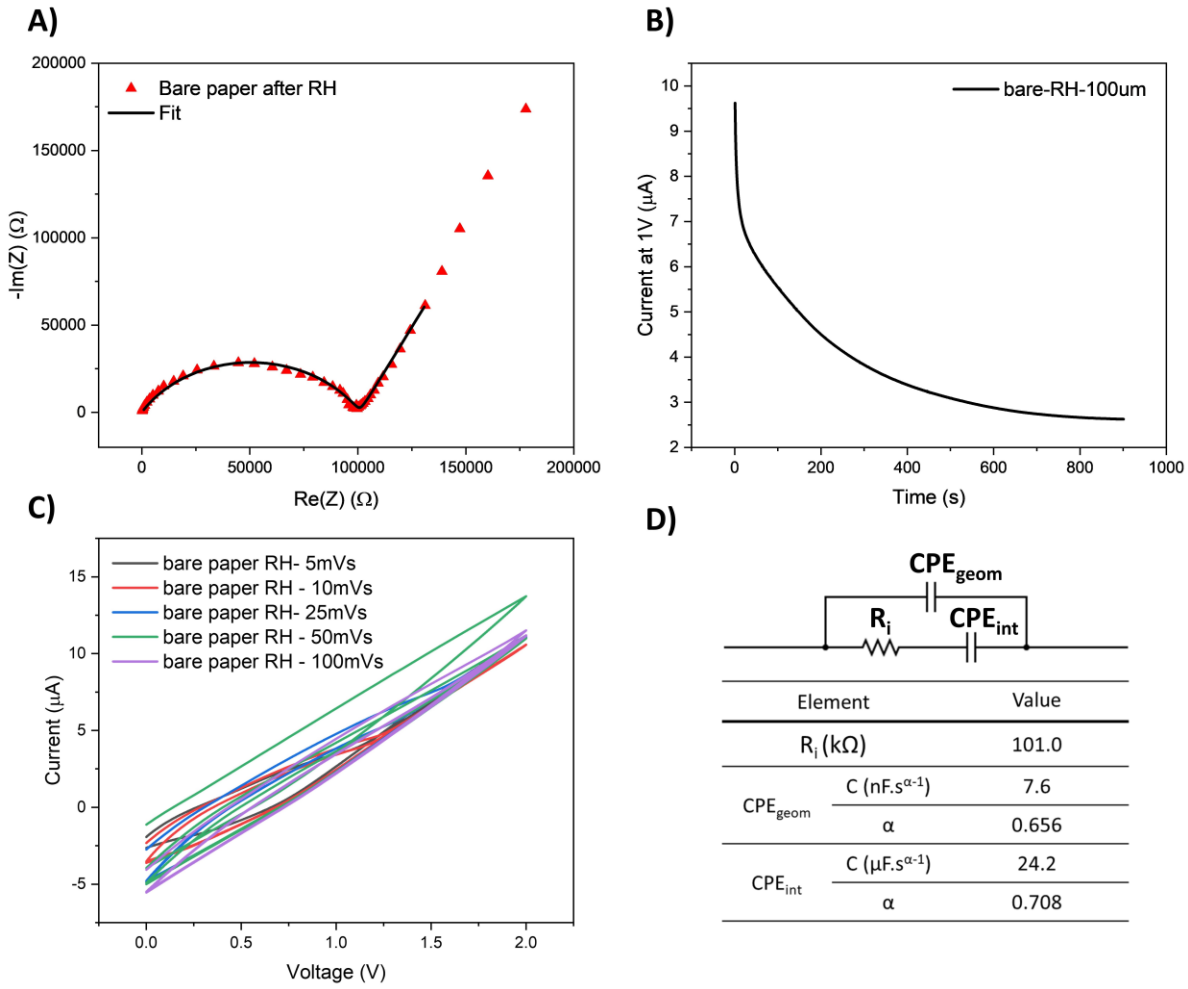

Element		Value
R_i (kΩ)		101.0
CPE_{geom}	C (nF.s$^{\alpha-1}$)	7.6
	α	0.656
CPE_{int}	C (μF.s$^{\alpha-1}$)	24.2
	α	0.708

Supplementary Figure 3. Electrical characterization of silver-electrode patterned paper after hydration. (A) Nyquist plot from impedance spectroscopy. (B-C) Current-voltage and transient response at 1 V of bare hydrated substrate, respectively. (D) Equivalent circuit model and data used to fit the Nyquist plot. R_i is the hydrated substrate (ionic) resistance and CPE_{geom} and CPE_{int}, are the constant phase elements representing the geometrical and interfacial capacitances of the system.

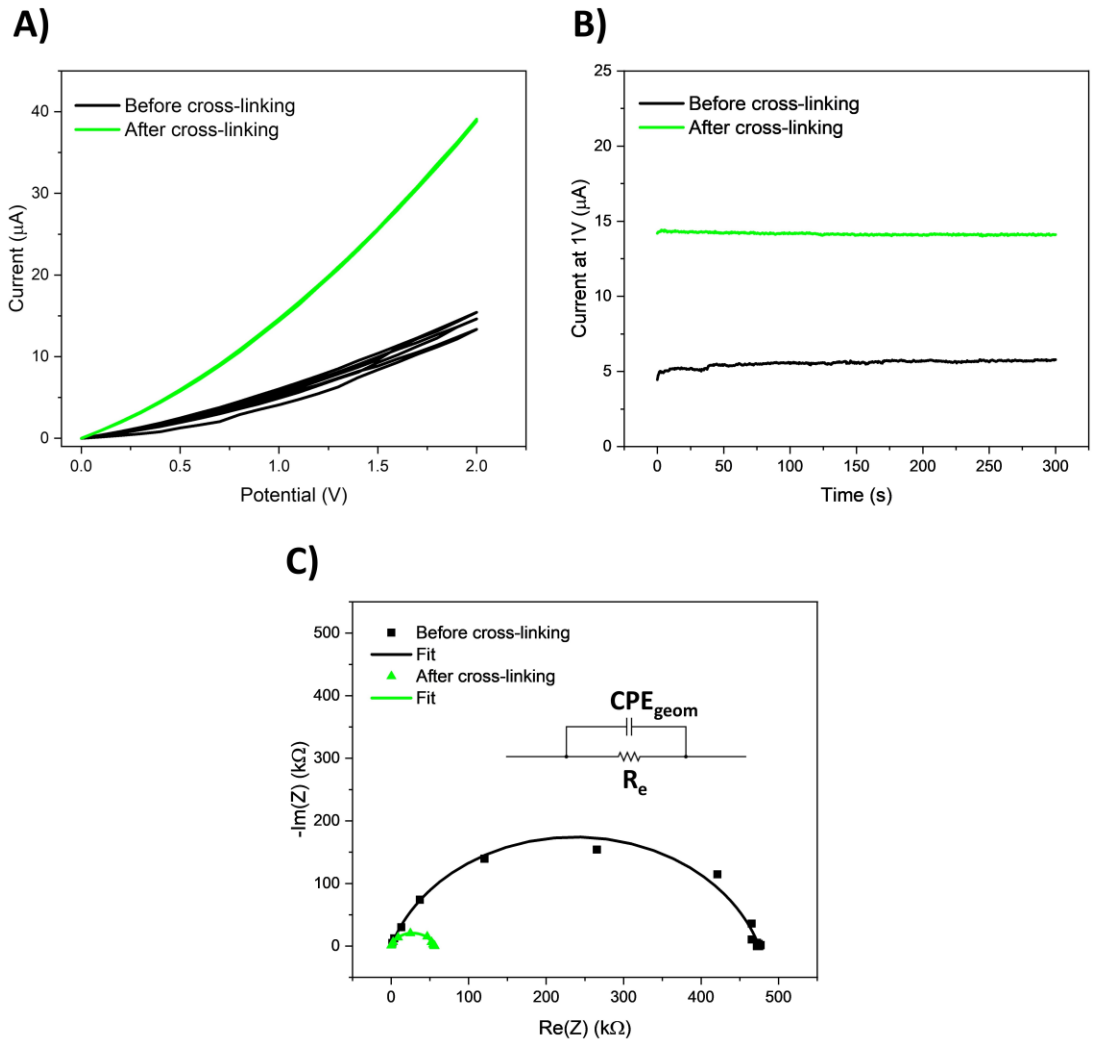

Supplementary Figure 4. Electrical characterization of Sepia melanin-shellac printed films before and after cross-linking (70 ˚C for 1 hr). (A) Three cycles of current-voltage response at 100 mV s^{-1} before and after cross-linking. (B) Transient current at 1 V. (C) Nyquist plot from impedance spectroscopy, respectively. The inset in (C) represents the equivalent circuit model used to fit the Nyquist plot. R_e is the film resistance and CPE_{geom}, is the constant phase element representing the geometrical capacitance of the system.

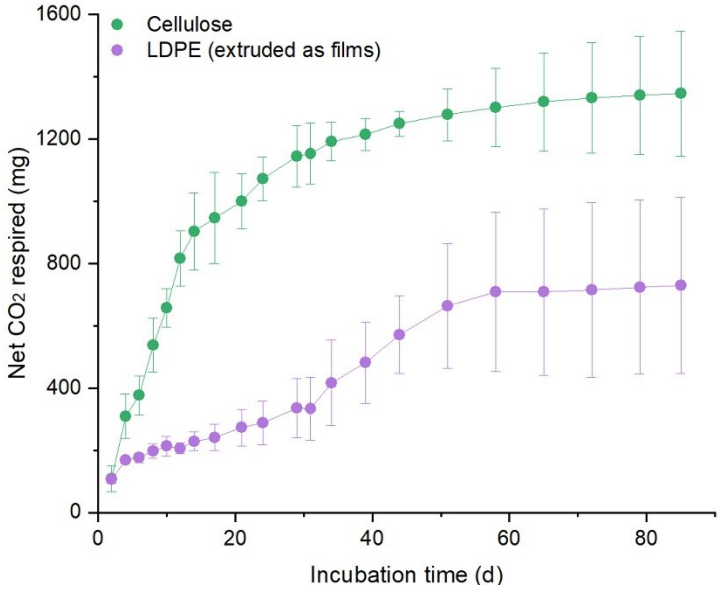

Supplementary Figure 5. Cumulative CO_2 respired of cellulose and LDPE and blank composts. Error bars indicate standard deviations of cumulative values (n = 3).

In our initial expectations, the CO_2 production curves of the reference compost and LDPE should have closely aligned. However, our experimental findings have unveiled a different and unexpected outcome.

On the one hand, this difference could be due to the presence of organic impurities within the LDPE material generated during the extrusion process. On the other hand, if we make the hypothesis of microbial degradation of LDPE, the pursuit of an unequivocal demonstration of an active microbial population capable of degrading LDPE film would surpass the scope of the present investigation.

The scenario where the measured CO_2 would be associated to the presence of organic impurities in the LDPE appears to be the most sound.

Our decision to reporting all experimental data is essential to ensure that the readers can grasp the context and credibility of our findings.

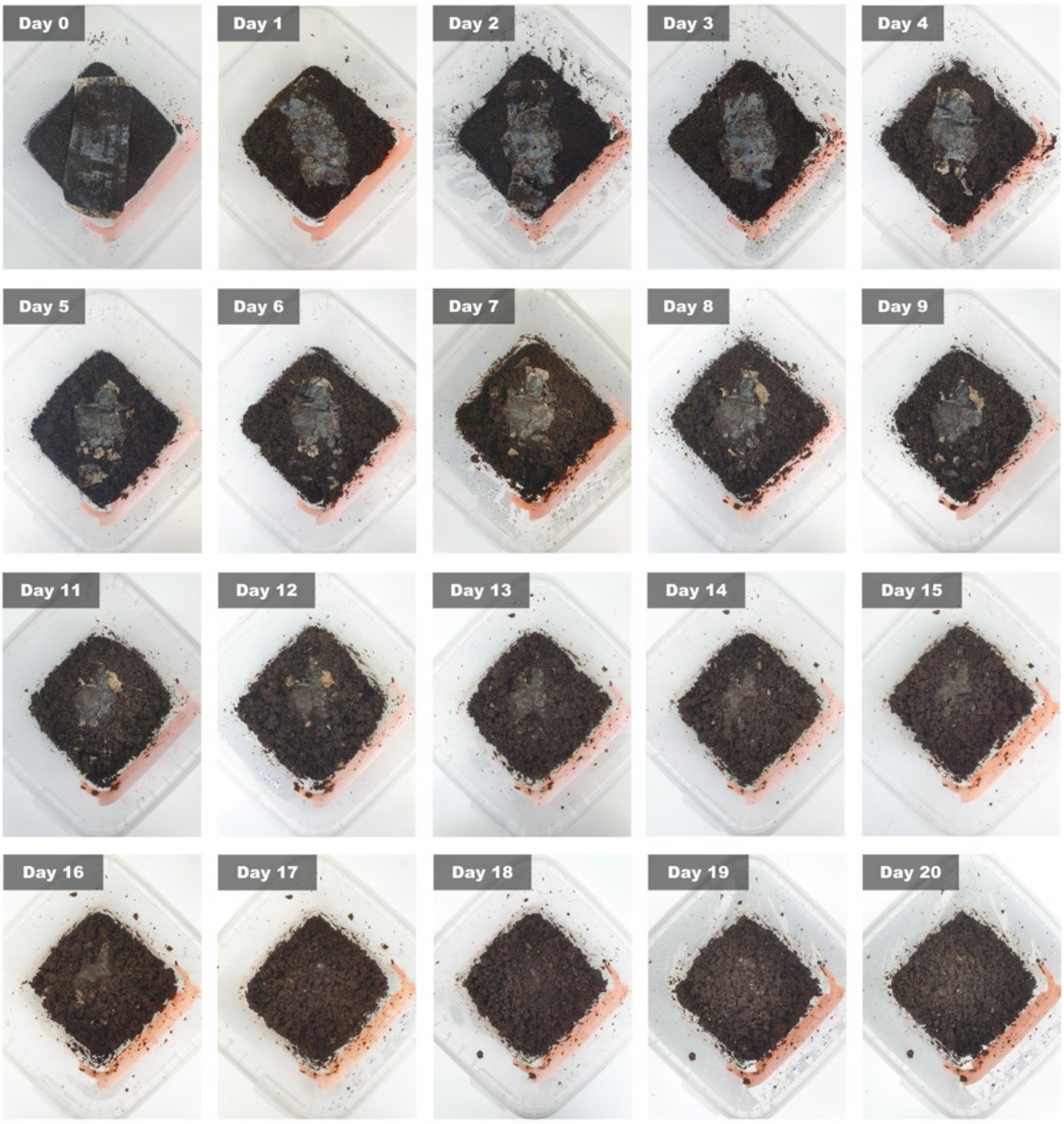

Supplementary Figure 6. Time-lapse optical images displaying top views of a microcosm experiment, demonstrating the rapid disintegration of the Sepia melanin-shellac printed film over a 20-day period under composting conditions (58 °C, 50% water content).

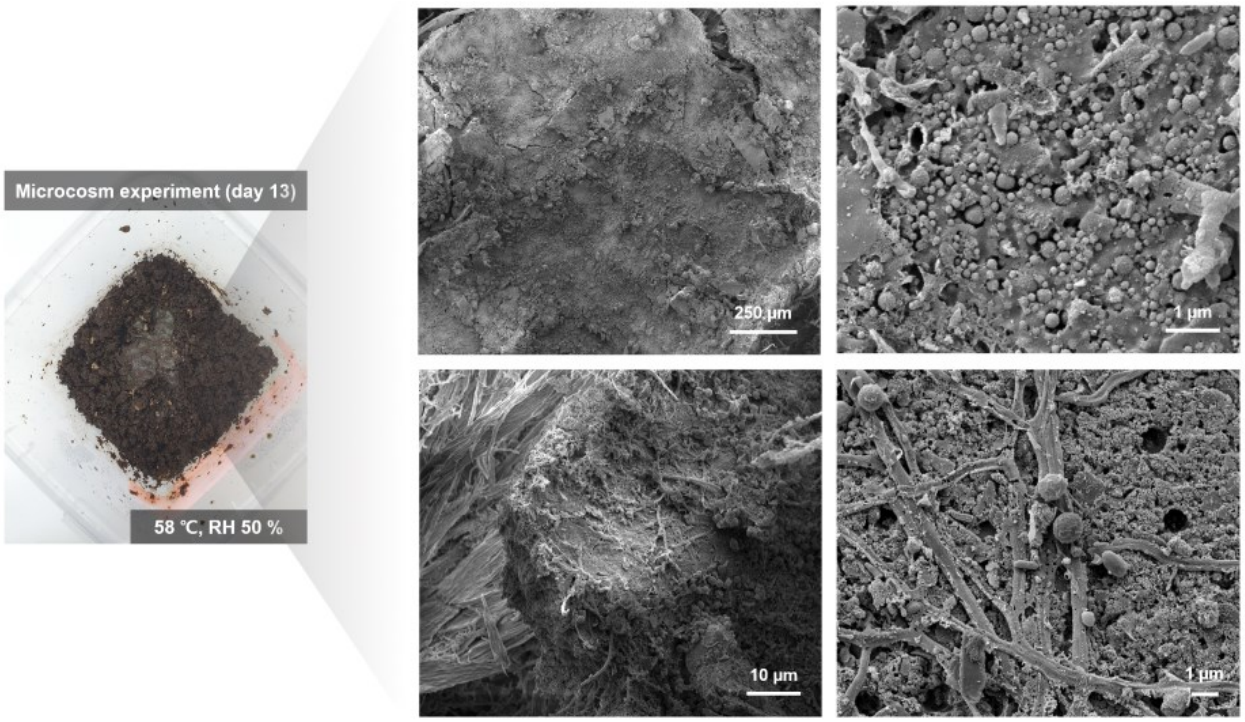

Supplementary Figure 7. SEM images of Sepia melanin-shellac printed film retrieved from a microcosm experiment after 13 days of incubation under composting conditions (58 °C, 50% water content).

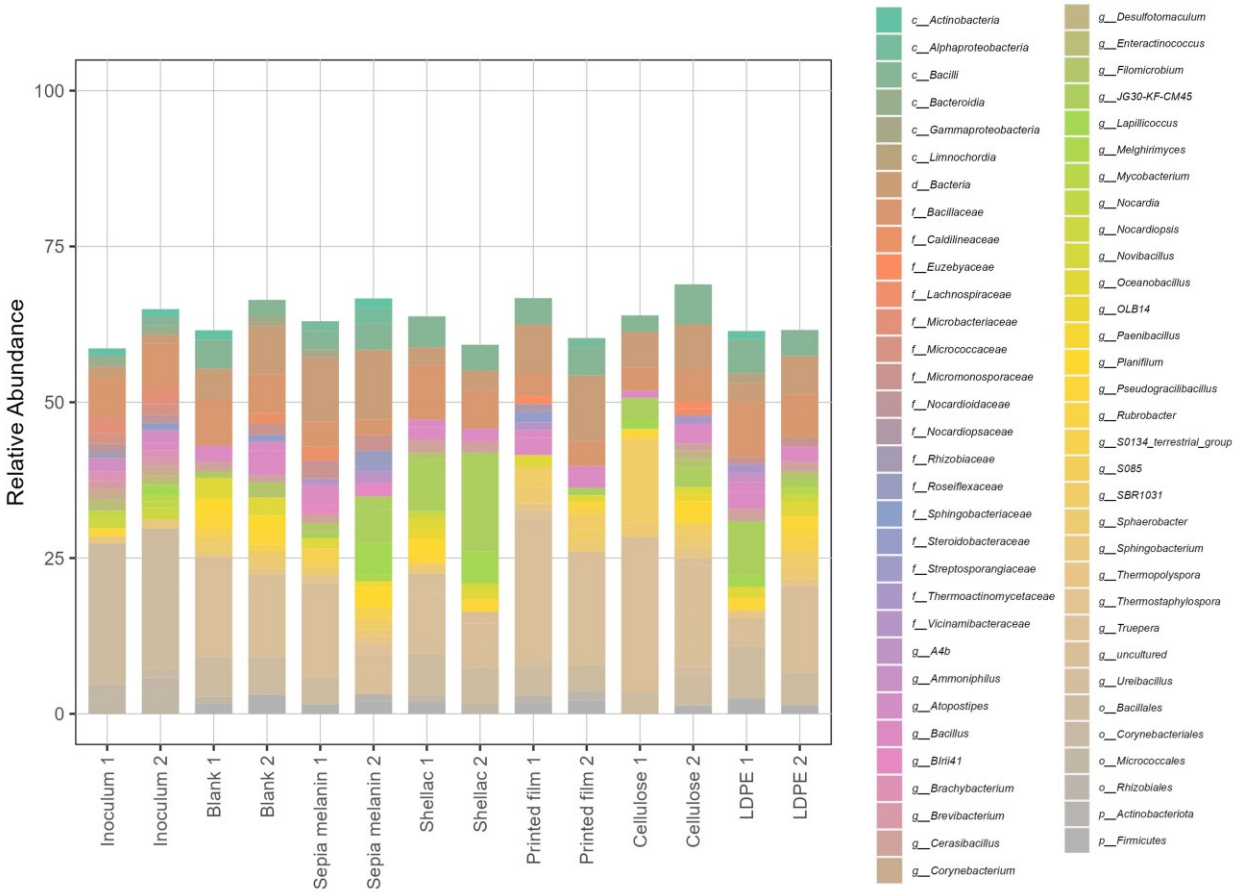

Supplementary Figure 8. Genus-level bacterial community diversity based on the 16s rRNA gene sequences representing more than 1.0 % of the amplicon sequences variants (ASVs) as the best BLAST hit, *i.e.*, the closest taxon.

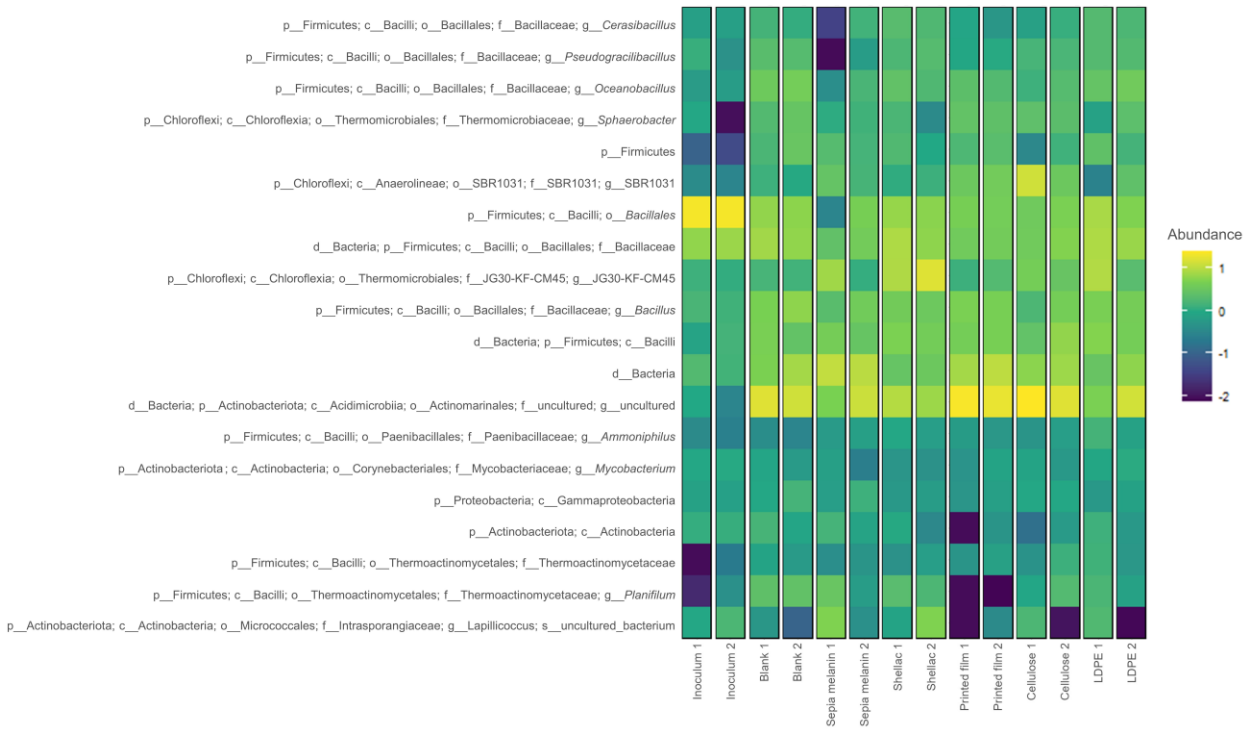

Supplementary Figure 9. Top 20 candidates at the genus level in the compost bacterial community visualized as a heatmap.

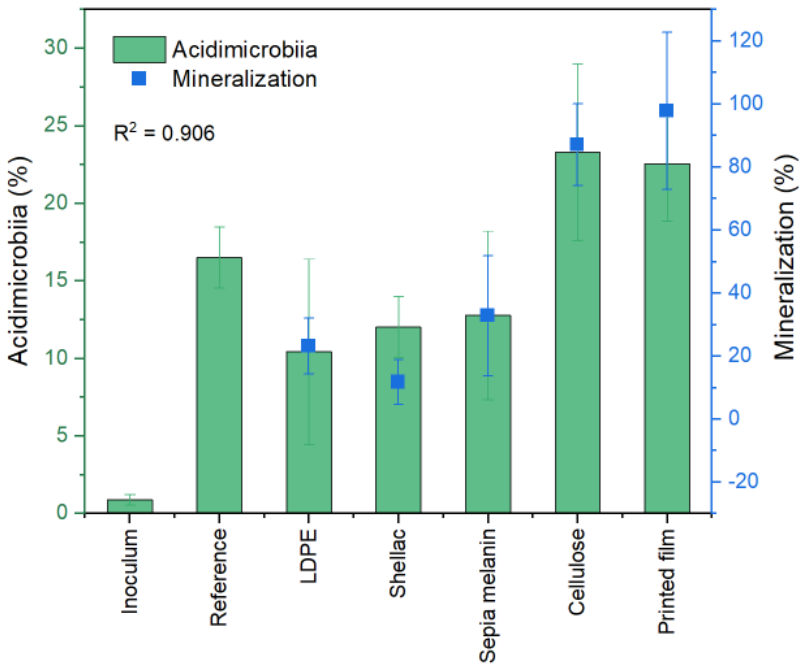

Supplementary Figure 10. Relative abundance of Acidimicrobiia in compost samples collected at the end of the 85-day biodegradation test, alongside test material mineralization levels. The abundance of Acidimicrobiia displayed a strong positive correlation with the test material mineralization (R^2 = 0.906), suggesting their crucial role in degrading specific materials like cellulose and Sepia melanin-shellac printed film.

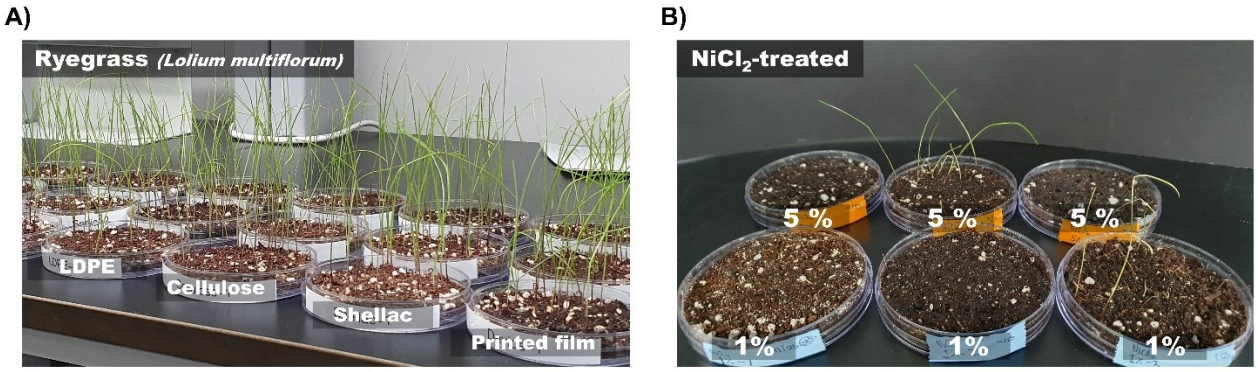

Supplementary Figure 11. Ecotoxicity evaluation using seeds of ryegrass (*Lolium multiflorum*). (A) Ryegrass germination with printed film, cellulose, shellac, and LDPE. (B) Significantly inhibited germination of ryegrass seeds with evident phenotypic damage in the presence of $NiCl_2$, a chemical known toxic compound.

Supplementary Figure 12. Ecotoxicity assessment using seeds marigold (*Tagetes erecta*). Marigold serves as the secondary bioindicator, highlighting that the composting of the printed film had no adverse effects on the germination of dicotyledon compared to the reference compost.

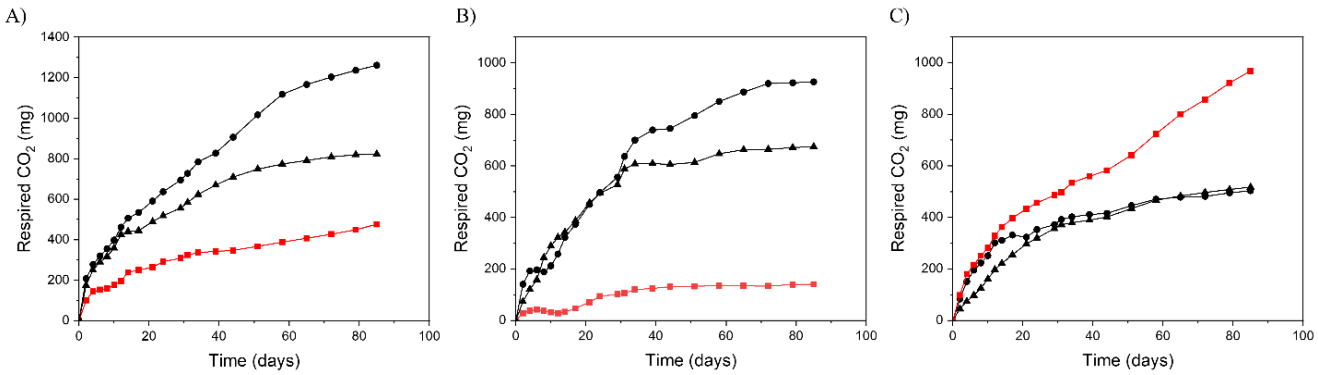

Supplementary Figure 13. Cumulative respired CO_2 for triplicates of **A)** Sepia melanin, **B)** Shellac and **C)** Reference compost. The red curves denote the 'outliers' in each set of data.

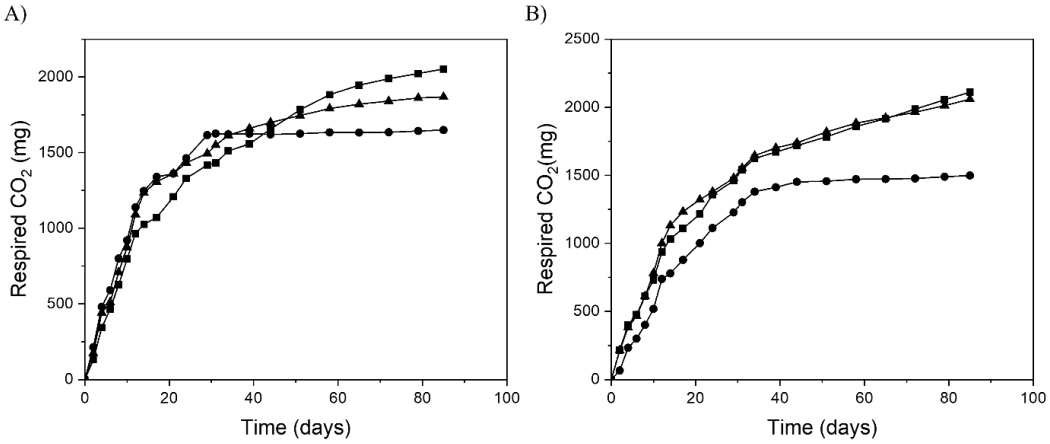

Supplementary Figure 14. Cumulative respired CO_2 for triplicates of **A)** Cellulose and **B)** Printed films.

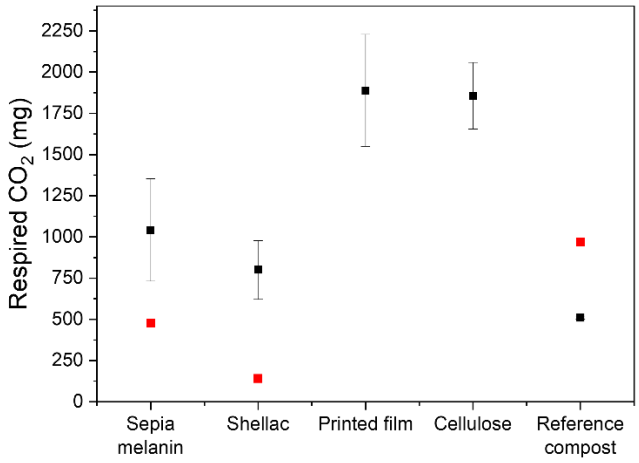

Supplementary Figure 15. Averages with their standard deviations and 'outlier' points for samples of Sepia melanin, Shellac, Printed films, Cellulose and Reference compost. There are no outliers for Printed films and Cellulose.

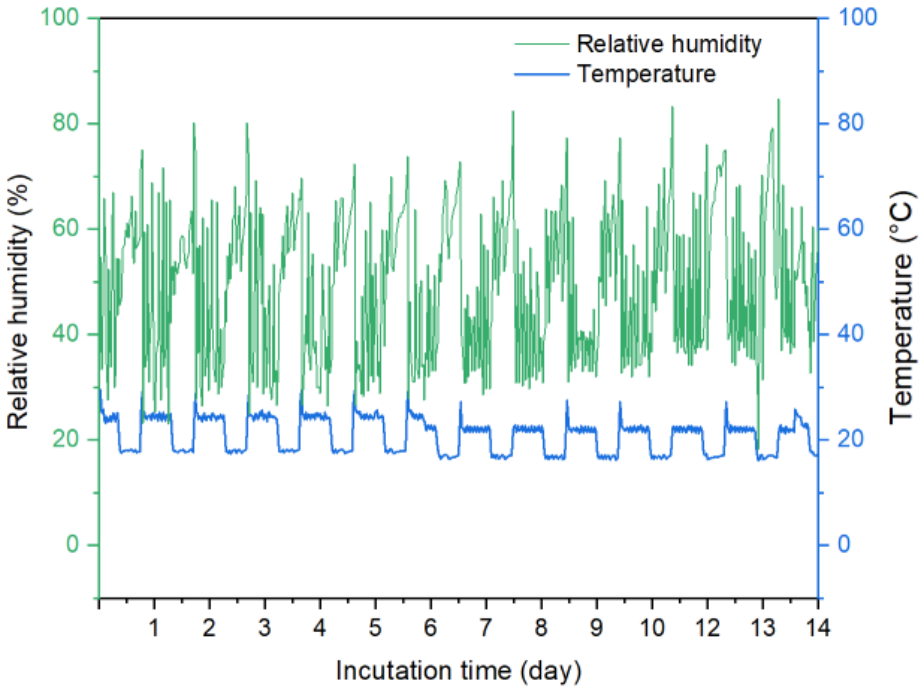

Supplementary Figure 16. Temperature and relative humidity profile during the germination test of *Lolium multiflorum*.

Supplementary Table S1. Bacterial richness and diversity indices of the compost upon completion of the 85-day biodegradation test. The values were evaluated based on amplicon sequence variants (ASVs) of 16S rRNA genes. Inoculum refers to a compost sample collected before the start of the biodegradation test, while reference compost designates a compost that was incubated without the addition of any test material.

Test material	Number of OTUs	Shannon index	Evenness
Inoculum (t_0)	376 ± 21	7.5 ± 0.1	0.87
Reference Compost	496 ± 29	8.2 ± 0.1	0.92
Sepia melanin	392 ± 72	8.0 ± 0.2	0.92
Shellac	372 ± 54	7.9 ± 0.2	0.92
Printed film	408 ± 37	7.8 ± 0.2	0.91
Cellulose	365 ± 68	7.6	0.89 ± 0.03
LDPE	437 ± 17	8.0	0.92

Table S2. Results of the phytotoxicity test. In this test, twenty seeds of Italian ryegrass (*Lolium multiflorum*) were incubated for 14 d while buried into compost samples collected at the conclusion of the 85-day biodegradation test. The germination test was conducted in triplicates.

Test material	Germination rate	Plant biomass (mg)	Shoot length (cm)
Reference Compost	0.95 ± 0.05	250.8 ± 17.9	10.1 ± 0.5
Sepia melanin	0.98 ± 0.03	290.1 ± 15.0	10.3 ± 0.7
Shellac	0.98 ± 0.03	303.1 ± 32.9	10.9 ± 0.9
Printed film	0.97 ± 0.03	290.1 ± 15.0	10.3 ± 0.3
Cellulose	0.98 ± 0.03	232.5 ± 43.1	10.7 ± 0.8
LDPE	0.95 ± 0.05	269.5 ± 47.7	10.9 ± 0.3
$NiCl_2$ -1	0.18 ± 0.18	28.5 ± 31.1	3.3 ± 3.0
$NiCl_2$ -5	0.10 ± 0.17	19.1 ± 33.1	2.5 ± 4.4

Supplementary Table S3: Summary of the respired CO_2 data as averages, standard deviations and outliers for Sepia melanin, Shellac, Printed film, Cellulose and Reference compost.

	Average (mg)	Std (mg)	Outliers (mg)
Sepia melanin	1041.8	310.1	476.5
Shellac	800.5	177.9	141.1
Printed film	1889.1	339.5	
Cellulose	1856.4	202.0	
Reference compost	510.3	9.7	968.7

References

[1] F. Ruggero, R. Gori, and C. Lubello, "Methodologies to assess biodegradation of bioplastics during aerobic composting and anaerobic digestion: A review," *Waste Manag Res*, vol. 37, no. 10, pp. 959–975, 2019, doi: 10.1177/0734242X19854127.

[2] G. X. Wang, D. Huang, J. H. Ji, C. Völker, and F. R. Wurm, "Seawater-Degradable Polymers—Fighting the Marine Plastic Pollution," *Adv Sci*, vol. 8, no. 1, pp. 1–26, 2021, doi: 10.1002/advs.202001121.

[3] S. Chinaglia, M. Tosin, and F. Degli-Innocenti, "Biodegradation rate of biodegradable plastics at molecular level," *Polym Degrad Stab*, vol. 147, no. December 2017, pp. 237–244, 2018, doi: 10.1016/j.polymdegradstab.2017.12.011.